Journal of Electrochemistry

Volume 29 | Issue 9

2023-09-28

Dependence of Heat Transfer Model on the Structure of Electrically Coil-Heated Microelectrodes

Ju Li
School of Henan Industry and Trade Vocational College, Zhengzhou, 451191, China;Key Laboratory of Targeting Therapy and Diagnosis for Critical Diseases, Henan Province, Key laboratory of Advanced Drug Preparation Technologies, Ministry of Education, Collaborative Innovation Center of New Drug Research and Safety Evaluation, School of Pharmaceutical Sciences, Zhengzhou University, Zhengzhou, 450001, China, liju1124@zzu.edu.cn

Sen Yang

Jian-Jun Sun
Ministry of Education Key Laboratory for Analytical Science of Food Safety and Biology; Fujian Provincial Key Laboratory of Analysis and Detection Technology for Food Safety, College of Chemistry, Fuzhou University, Fuzhou, Fujian 350108, China, jjsun@fzu.edu.cn

Recommended Citation
Ju Li, Sen Yang, Jian-Jun Sun. Dependence of Heat Transfer Model on the Structure of Electrically Coil-Heated Microelectrodes[J]. *Journal of Electrochemistry*, 2023 , 29(9): 2203211.
DOI: 10.13208/j.electrochem.2203211
Available at: https://jelectrochem.xmu.edu.cn/journal/vol29/iss9/4

ARTICLE

Dependence of Heat Transfer Model on the Structure of Electrically Coil-heated Microelectrodes

Ju Li [a,b,*], Sen Yang [b,c], Jian-Jun Sun [c,*]

[a] School of Henan Industry and Trade Vocational College, Zhengzhou, 451191, China
[b] Key Laboratory of Targeting Therapy and Diagnosis for Critical Diseases, Henan Province, Key Laboratory of Advanced Drug Preparation Technologies, Ministry of Education, Collaborative Innovation Center of New Drug Research and Safety Evaluation, School of Pharmaceutical Sciences, Zhengzhou University, Zhengzhou, 450001, China
[c] Ministry of Education Key Laboratory for Analytical Science of Food Safety and Biology, Fujian Provincial Key Laboratory of Analysis and Detection Technology for Food Safety, College of Chemistry, Fuzhou University, Fuzhou, Fujian, 350108, China

Abstract

Electrically heated microelectrodes have gained much attention in electroanalytical chemistry in recent years. It has been shown that the promotion of mass transport and reaction kinetics at high-temperatures often results in increased current signals. However, there is no study about the heat transfer inner the microelectrodes which is necessary for the design and operation for microsensors. This report introduces a finite element software (COMSOL) to analyze the factors that influence the surface temperature (T_s), which is crucial for the heating ability of micro-disk electrodes with coils. Distances between the electrode surface and the bottom of the heated copper wire also have a good linear relationship with T_s ($R^2 = 1$). Considering the cost, 25-mm length of the gold wire is enough to obtain a relatively high T_s. In addition, the highest T_s can be obtained when the electrode material is gold and the diameter of the gold disk is 0.2 mm. The relationship of diameters of heated copper wires with currents to obtain different temperatures has also been studied. It is expectable that the simulation results can be used to significantly help the design and operation of electrically heated microsensors in practical applications.

Keywords: Electrically heated microelectrodes; Heat transfer; Micro-disk; Coil-heated; Model; COMSOL; Temperature distribution

1. Introduction

During the last two decades, electrically heated microelectrodes invented by Gründler's group have attained considerable attention in electroanalytical chemistry [1−3]. The symmetrical construction of the electrode allows one to raise the electrode temperature to several tens of degrees centigrade or more above the solution boiling point, while keeping the solution temperature almost unchanged by using a high frequency alternating current, and to perform electroanalytical measurements by applying a direct current polarization at the same time [4−6]. Principles and analytical applications of them can be found in reviews [7−11]. There are many advantages for them, such as affecting thermodynamic and kinetic parameters of the electrode reaction, accelerating the redox reaction rates, fast control of electrochemical reaction temperature. In addition, no organic electrolyte, which is harmful for human body, is needed in studying the electrochemical reaction on the electrode surface temperature (T_s) higher than boiling point, and energy saving can be realized [12−21].

Coil-heated micro-disk electrodes have been used as micro-biosensors in bioanalytical area. The dramatic temperature effect on the adsorptive accumulation of luteolin has been demonstrated using a pencil lead micro-disk electrode [22]. The

Received 21 March 2022; Received in revised form 27 April 2022; Accepted 28 April 2022
Available online 7 May 2022

* Corresponding author, Ju Li, Tel: (86-371)67781891, E-mail address: liju1124@zzu.edu.cn.
* Corresponding author, Jian-Jun Sun, Tel: (86-591)22866136, E-mail address: jjsun@fzu.edu.cn.

https://doi.org/10.13208/j.electrochem.2203211

greatly enhanced electrocatalytic activity of hemin/G-quadruplex horseradish peroxidase-mimicking DNAzyme for H_2O_2 reduction with elevated electrode temperature has also been reported by using gold particle modified heated copper [23] and gold electrodes [24]. In addition, Exonuclease III for signal amplification with an elevated temperature in electroanalytical chemistry has been achieved using a heated gold disk electrode [25]. However, there is no study about the heat transfer for electrically heated microelectrodes which is necessary for the design and operation of electrodes, especially for the application in bioanalysis.

In contrast to electrochemical experiments which usually provide only information about the average temperature of the electrode surface or the bulk solution, numerical simulations give more details for the electrode surface. Gründler has explored the heat transfer and mass transfer coupling process for a direct continuous heating wire electrode by establishing a hot wire electrochemical model [26]. The mass transfer and heat transfer for high-frequency AC heated microelectrode solutions have been studied by Baranski and Boika's group through theoretical calculations and numerical simulations [27−29]. The heat transfer inner a temperature controllable electrode with a relatively large electrode surface (3−5 mm in diameter) has also been studied [19]. In addition, many other works have been done for temperature calculations and simulations of heated electrodes [30−35].

In this work, we introduce a finite element software (COMSOL) to analyze the factors that influence the surface temperature (T_s). Heat transfer in a coil-heated micro-disk electrode (CHMDE) that works in a three-electrode electrochemical cell is analyzed and modeled. This could lead to much more reliable and sensitive heated micro-disk sensors.

2. Materials and methods

2.1. Materials

Chemical agents of analytical grade, polyoxymethylene, gold wire (thickness ca. 0.5 mm) and copper wire (thickness ca. 70 μm) were purchased from Sinopharm Chemical Reagent Co., Ltd. Electric wires were obtained from Shenzhen Zaoxin Electronics Co., Ltd. Aqueous solutions were prepared with purified water (≥18 MΩ·cm) from a Millipore Milli-Q system (Research Scientific Instruments Co., Ltd., China). Thermal grease (YS910), as a good thermal conducting and Insulating material, was bought from Shenzhen Huanengzhiyan Co., Ltd. Epoxy resin (DEYI) was purchased from Changsha Baxiongdi Adhesive Co., Ltd.

2.2. Apparatus

Digital multimeter (VC890D) was obtained from Xi'an victor Instrument Co., Ltd. Direct current power (TPS300P) was bought from Shenzhen Atten Technology Co., Ltd. Electrochemical measurements were performed with an electrochemical potentiostat (CHI660D, Chenhua, China). COMSOL5.3a software was purchased from the COMSOL Corporation (Shanghai, China). An electrochemical cell with a traditional three-electrode configuration was used (Fig. 1b). A coil-heated micro-disk electrode (Fig. 1a) was used as the working electrode. A platinum wire electrode (Jinhuice.com, Nanjing, China) was used as the counter electrode and a saturated calomel electrode (Jinhuice.com, Nanjing, China) as the reference electrode. The cell was kept in ice-water bath, maintaining the temperature of the bulk solution.

2.3. Temperature calibration

The relationship between time and potential of a gold coil-heated micro-disk electrode (Au-CHMDE) in 5 $mmol\cdot L^{-1}\cdot K_3Fe(CN)_6$ + 0.1 $mol\cdot L^{-1}\cdot KCl$ solution is shown in Fig. 1c. The temperature of the electrode surface was measured by following the temperature-dependent change of the open-circuit potential of a reversible redox couple [4], and the temperature potential coefficient of this redox couple is 1.56 $mV\cdot K^{-1}$ [3]. The temperature rise of the electrode surface can be calculated using Equation (1) as follows,

$$\Delta T_1 = (E - E_0)/1.56 \quad (1)$$

where ΔT_1 (°C) is the temperature rise, E ($mV\cdot K^{-1}$) is the potential applied to the electrode when the current is presented, while E_0 ($mV\cdot K^{-1}$) is the potential applied to the electrode when the current is zero.

3. Results and discussion

3.1. Geometric model and characterization of Au-CHMDE

The fabrication of Au-CHMDE was similar to the heated gold disk electrode designed by Wu et al. [25]. Its geometric model can be described schematically (Fig. 1a) as a graphic of axial symmetry constituting four distinct areas. An electric copper wire with its rubber coat was in the upper part of the Au-CHMDE. The polyoxymethylene coat was

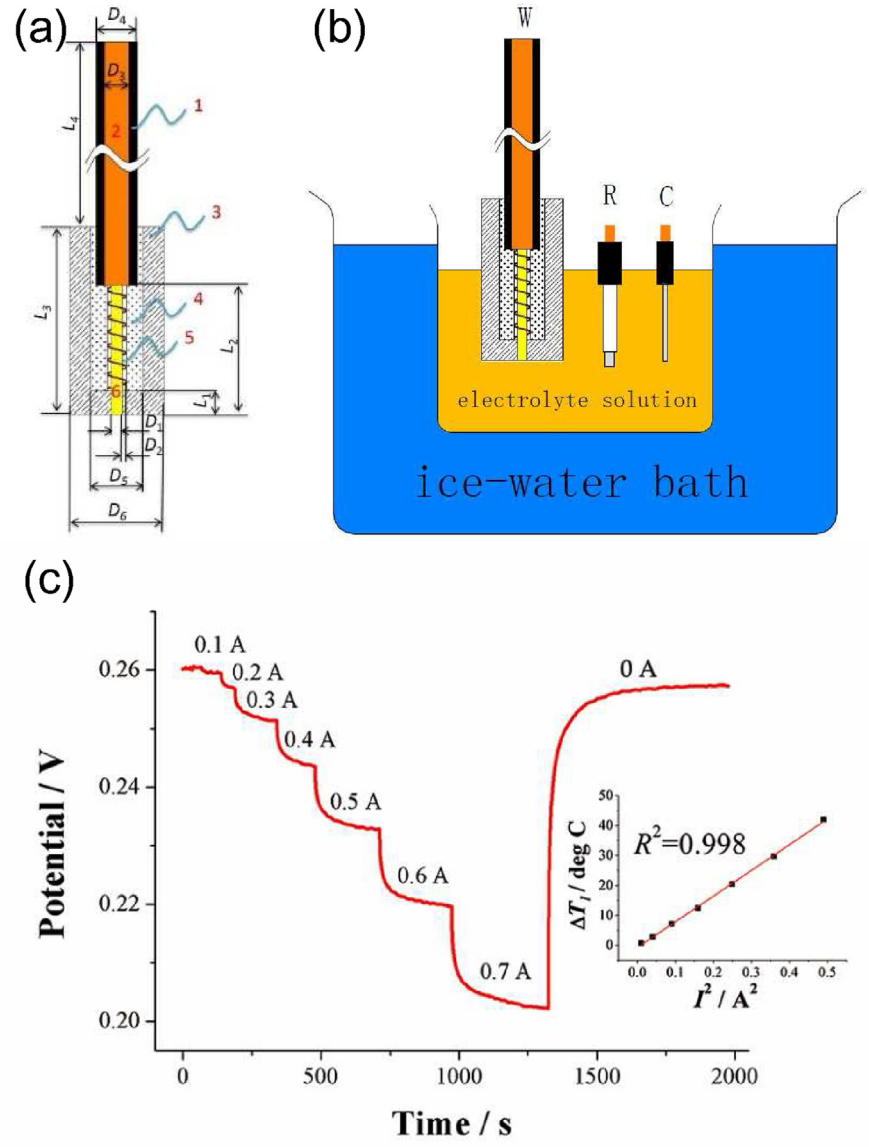

Fig. 1. The structure and experiment setup of a gold coil-heated micro-disk electrode (Au-CHMDE). (a) Schematic description of the heat gold wire electrode (1: the rubber sleeve of the electric copper wire, 2: the electric copper wire, 3: polyoxymethylene, 4: epoxy resin, 5: the heated copper wire, 6: the gold wire, D_1 and D_2 represent the diameters of the gold wire and heated copper wire, respectively. D_3 and D_4 represent the diameters of the electric copper wire and its rubber sleeve, respectively. D_5 and D_6 represent the diameters of the epoxy resin and polyoxymethylene, respectively. L_1 represents the distance from the bottom of the heated copper wire to the electrode surface. L_2 represents the length of the gold wire. L_3 represents the length of the polyoxymethylene coat. L_4 represents the length of the copper wire out of the polyoxymethylene coat; (b) The Au-CHMDE setup. W, R, and C represent the working electrode, the reference electrode, and the counter electrode, respectively; (c) Potential-time curve of the heated gold wire electrode (Au-CHMDE) in 5 mmol·L^{-1} $K_3Fe(CN)_6$ + 0.1 mol·L^{-1} KCl solution. (Inset: Relationship between temperature rise (ΔT_1) at Au-CHMDE (D_1 = 0.5 mm) and the square of heating current in the solution).

in the lower part of the Au-CHMDE. A gold wire was contacted with the bottom of the copper wire. A thinner double parallel copper enameled wire connected with a direct current power was twined around the gold wire as the heater. The resistance of the copper wire was detected to be ca. 2.0 Ω by using a digital multimeter. The epoxy resin was fully filled in the gap between the gold wire and the polyoxymethylene coat.

The experiment setup of Au-CHMDE is shown in Fig. 1b, the Au-CHMDE was placed in the electrolyte solution surrounded by ice-water bath to keep the temperature of the bulk solution approximately 0 °C.

The open-potential for Au-CHMDE was changed when applying different direct currents to the heated copper wire. T_s can be calculated by monitoring the change in the potential in

potassium ferricyanide with the temperature-potential coefficient (Fig. 1c). The result (the inset in Fig. 1c) depicts that the temperature rise is linear with the square of the heating current. And the equation of the fitting curve is $\Delta T_1 = -0.7462 + 85.8742I^2$ ($R^2 = 0.998$), and ΔT_1 (°C) is the temperature rise, I (A) is the current applying to the electrode.

3.2. Heat transfer in Au-CHMDEs

3.2.1. The establishment of the theoretical model

To verify the robustness of the numerical model, a comparison between the experiment data and the simulated data were carried out. The physical dimensions and environment of the electrode are detected as $D_1 = 0.5$ mm, $D_2 = 70$ μm, $D_3 = 1$ mm, $D_4 = 1$ mm, $D_5 = 5$ mm, $D_6 = 6$ mm, $L_1 = 2$ mm, $L_2 = 15$ mm, $L_3 = 80$ mm, $L_4 = 350$ mm. The temperature of the water under the electrode surface is assumed to be 0 °C due to the use of the ice-water bath. Because of the low temperature, the convective heat transfer coefficient between the electrode surface and the water is supposed to be 200 $W \cdot m^{-2} \cdot K^{-1}$. When the applied current for the heated copper wire is larger than 0.4 A, leading to the rise of temperature, the convective heat transfer coefficient between the electrode surface and the water is supposed to be 300 $W \cdot m^{-2} \cdot K^{-1}$. And the convective heat transfer coefficient between the electrode surface and the water is supposed to be 12.5 $W \cdot m^{-2} \cdot K^{-1}$. The temperature around the electrode side is assumed to be 18.5 °C which is the average of the bottom temperature of electrode side (12 °C) and top temperature of electrode side (25 °C). And the temperature around the copper wire is the room temperature (25 °C).

Then the model is solved using COMSOL, which was bought from the COMSOL Corporation. The simulated temperature rise ΔT_2 can be defined as follows,

$$\Delta T_2 = T\text{-}T_0 \quad (2)$$

wherein T is the temperature when applying different currents to the heated copper wire. T_0 is the temperature simulated to be 2.8 °C when applying no current to the heated copper wire.

When applying different currents, different temperatures were calculated as shown in Fig. 2a. And the comparison between the temperature rise (ΔT_1) obtained by the experiment and the temperature rise (ΔT_2) simulated by COMSOL is implemented. The linear slope of the fitting line of k is 0.9964 ($R^2 = 0.9924$), which shows excellent consistence with those of the model and experiment on the error below 0.4%. Thus, T_s and the heat transfer inside the electrode based on this model can be studied.

As shown in Fig. 2b, T_b is the bottom temperature of the heating copper wire and T_s is the temperature of the electrode surface. The temperature difference ($\Delta T_3 = T_b - T_s$) between the bottom of the heating copper wire and the electrode surface has a good linear relationship with the square of heating current (I^2). And the fitting line for the relationship can be described as follows,

$$\Delta T_3 = 0.098 + 3.6545I^2 \ (R^2 = 0.9977) \quad (3)$$

Hence, the temperature difference between the bottom of the heating copper wire and the electrode surface can be calculated according to the heating current, which is helpful for the design of electrically heated electrodes in practical applications.

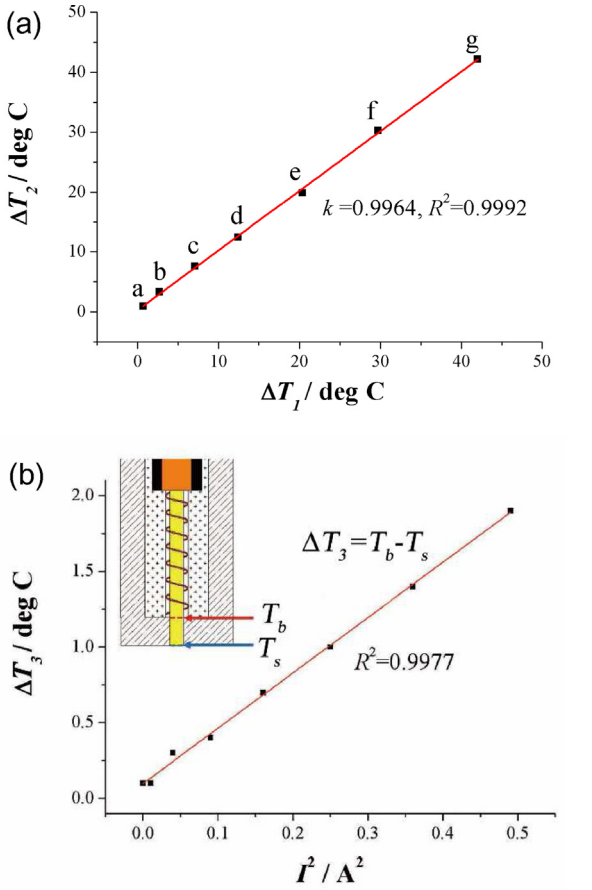

Fig. 2. (a) The comparison between the temperature rise (ΔT_1) obtained by experiment and the temperature rise (ΔT_2) simulated by COMSOL when applying different currents to the heated copper wire. From a to g, the currents varied from 0.1 A, 0.2 A, 0.3 A, 0.4 A, 0.5 A, 0.6 A, 0.7 A; (b) The relationship between the simulated temperature difference (ΔT_3) and the square of heating current. (Inset: the graphic representation showing T_s, T_b, and ΔT_3.)

3.2.2. Temperature distribution for the Au-CHMDE

When the heating current was 0.7 A, the heating power was 0.98 W owing to 2 Ω resistance of the heated copper wire. The convective heat transfer coefficient between the electrode surface and the water is assumed to be 300 $W \cdot m^{-2} \cdot K^{-1}$ as discussed before. And the temperature distribution for the Au-CHMDE is shown in Fig. 3, which is helpful for understanding the heat transfer in the inner electrode.

The area around the heated gold wire is the hottest and the temperature decreased from the center to the side (Fig. 3a and b). Fig. 3c depicts the temperature profile along the surface radius direction and the temperature distribution at the electrode surface, indicating that the temperature of the whole bottom face of the gold wire is equal. In addition, the temperature decreased from the center to the edge as same as in Fig. 3a and b. As shown in Fig. 3d, the temperature raised and then decreased to the room temperature from the bottom to the top of the electrode along the axle wire. ΔT_3 is approximately 1.9 °C and the temperature difference between the electrode surface and the top of the gold wire is approximately 11.1 °C.

3.3. Factors that influence the electrode surface temperature

Fig. 4 shows the factors that influence T_s when applying constant current to the heated copper coil. All the parameters used in the heat transfer model are the same as above except the changing factors. Studying the distance between the electrically heated copper coil and the electrode surface

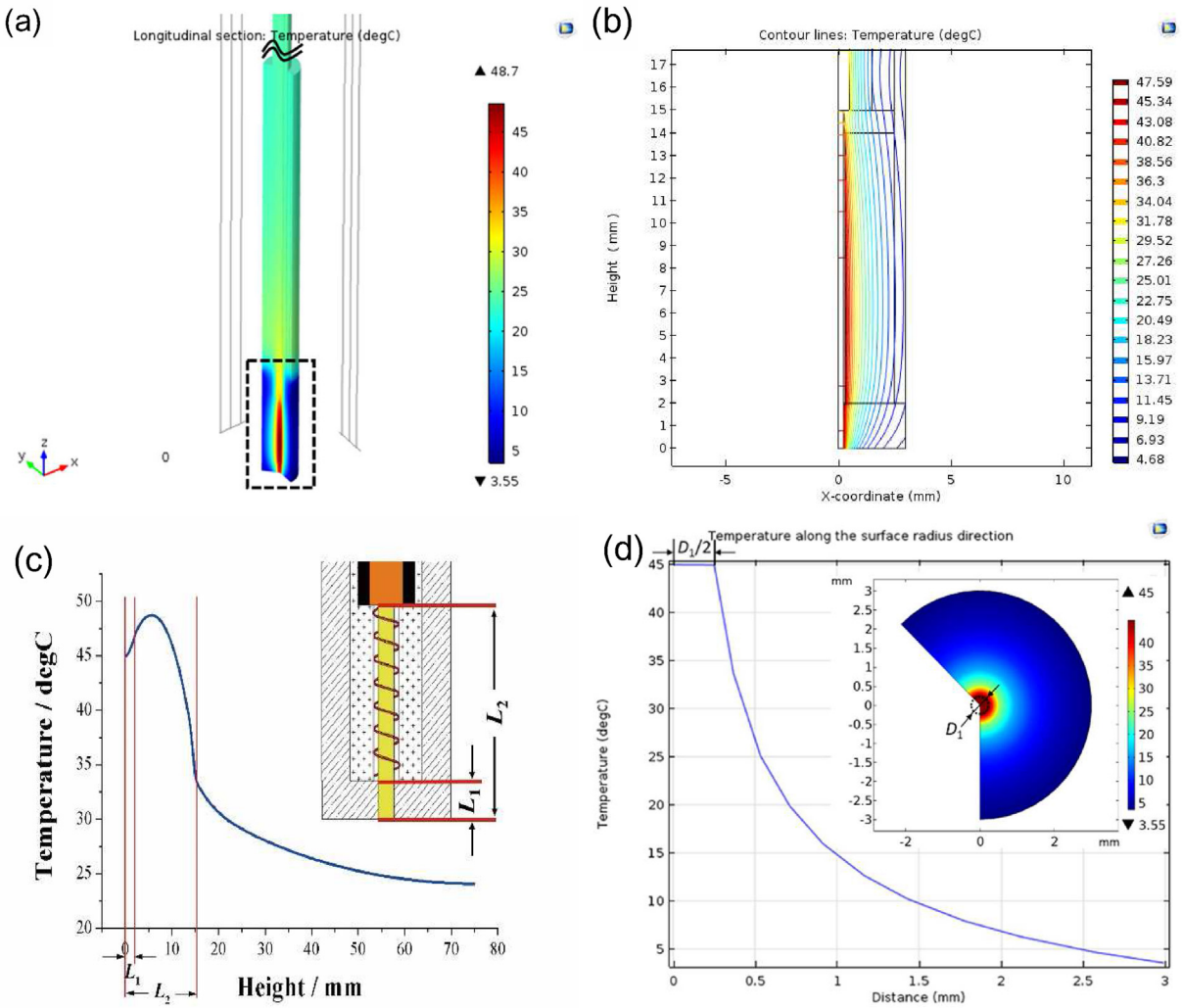

Fig. 3. Temperature distribution for the Au-CHMDE when 0.7 A current (0.98 W) was applied to the heated copper wire. (a) The temperature distribution for the Au-CHMDE at longitudinal section; (b) The temperature contour lines for the Au-CHMDE as indicated by the dashed box in Fig. 1a at longitudinal section; (c) Temperature profile along the surface radius direction (the inset: the temperature distribution at the electrode surface), D_1 is the diameter of gold wire; (d) Temperature profile along the axle wire of Au-CHMDE (Inset: the graphic representation showing L_1 and L_2).

is necessary to the fabrication of the electrode. Therefore, its effect on T_s was studied. T_s has a very good linear relationship with the distance L_1 (mm) between the bottom of the heating copper wire and the electrode surface (Fig. 4a). In addition, the equation of the fitting line is $T_s = 54.6 - 4.8L_1$, ($R^2 = 1$). Therefore, when there is no distance between the electrode surface and the heated copper wire, which indicating $L_1 = 0$, thus, T_s is 54.6 °C. When L_1 increases per 1 mm, T_s decreases 4.8 °C. Therefore, within the range suitable for multiple polishing of the electrode, reducing the distance between the electrically heated copper coil and the electrode surface as much as possible helps to obtain a higher T_s.

Gold is a commonly used electrode material and is relatively expensive. Studying the effect for the length of the gold wire (L_2) on T_s can help save cost and achieve the best heating effect. Fig. 4b shows the relationship between T_s and L_2, indicating that L_2 has little impact on T_s when L2 varies from 15 mm to 45 mm. As L_2 increasing, T_s is increasing gradually. However, when L_2 is 25 mm, T_s tends to be stable. In addition, the Boltzmann fit of the curve is described as,

$$T_s = 47.1 - \frac{419.4}{1 + e^{(L_2+1.0)/3)}} \quad (4)$$

Similarly, studying the effect for the diameter of the gold wire on the surface temperature of the electrode can also help to save cost and achieve the best heating effect. The relationship between T_s and the diameter of the gold wire (D_1) is shown in Fig. 4c. When D_1 is 0.2 mm, the electrode surface is hottest. Three factors may be considered: the heat capacity of the gold wire, the heat conduction of the gold wire and the convection cooling between the gold wire and the water. Since $D_1 = 0.2$ mm is thinner, resulting in the smaller heat capacity, the gold wire could be heated to a higher temperature. In addition, the cross-sectional area is moderate, it has the faster heat conduction ability and the convection cooling with water is slower. In the future work, when making a CHMDE, 0.2-mm gold wire should be chosen as the electrode material if needing a higher T_s.

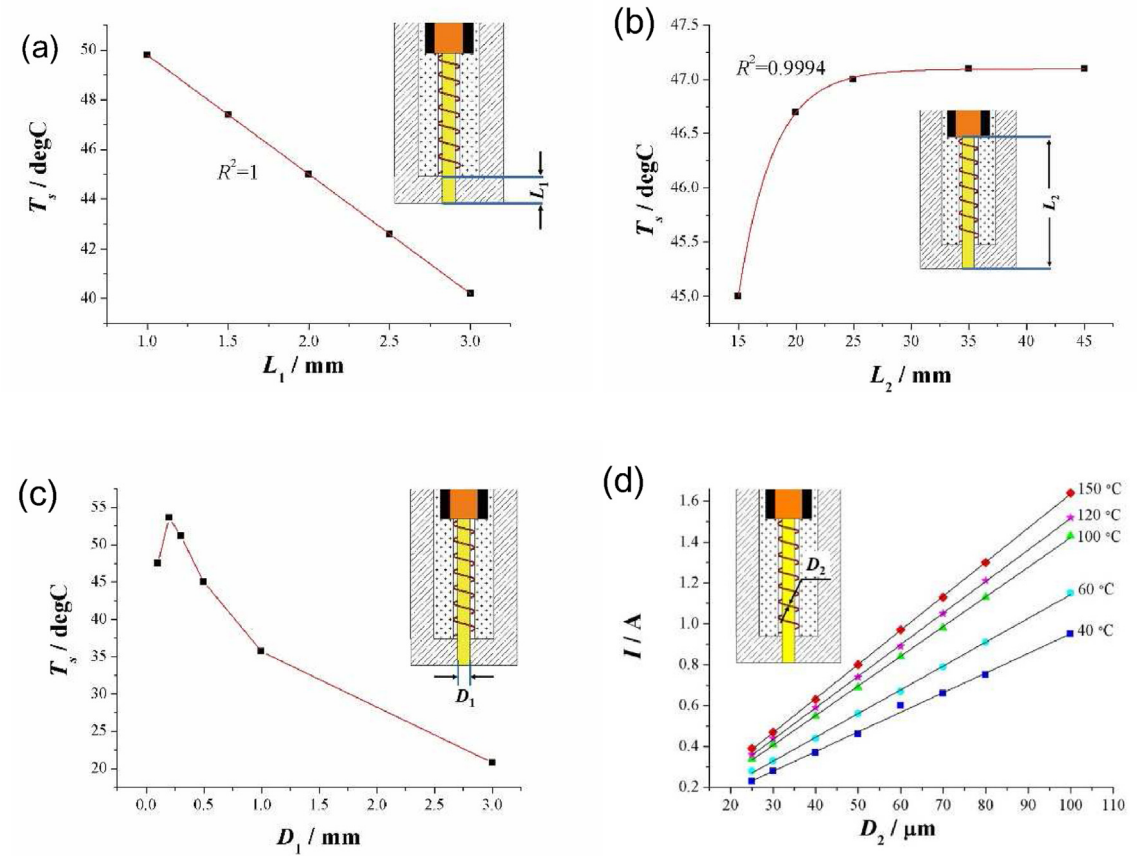

Fig. 4. Factors that influence T_s *when applied constant power to the heated copper wire. (a) The relationship between* L_1 *and* T_1*. (Inset: the graphic representation of* L_1*); (b) The relationship between* L_2 *and* T_1*. (Inset: the graphic representation of* L_2*); (c) The relationship between* D_1 *and* T_1*. (Inset: the graphic representation of* D_1*); (d) The relationship of diameters of heated copper wires and currents to obtain different temperatures. (Inset: the graphic representation of* D_2*).*

Due to its good thermal conductivity and large thermal resistance, copper coil is often used to heat the electrode. To investigate the acquired currents to achieve a certain T_s for different heated copper wires, the relationship of diameters of heated copper wires and currents to obtain different temperatures was studied as shown in Fig. 4d. They all have a good linearity as evident in the figure. At different electrode surface temperatures, the increase in the diameter of the copper wire requires a higher heating current. The diameter of the heated copper coil has a good linear relationship with the heating current as listed in Table 1.

The higher T_s, the better the linearity. The data can be used to guide the selections of a suitable size for the heated copper wire and appropriate current for an electrode to achieve a certain T_s. The results of the theoretical simulation can be used to assist the design and operation of heated gold disk electrodes in practical applications.

The electrode material has a significant influence on the electrochemical reaction and the electrode heating ability. Therefore, it is useful for researchers to choose a proper electrode material to study the relationship between the T_s and the electrode material. Table 2 shows the T_s for different electrode materials when applied constant power to the heated copper wire. The gold electrode obtained the highest T_s (45 °C), while the silver, copper and graphite electrodes achieved the T_s higher than 44.5 °C. However, the T_s values of nickel and platinum electrodes were relatively lower.

This may be explained by two factors. One is that the lower thermal conductivity results in the worse heat dissipation ability from the heating copper wire to the aqueous solution. Because of the lowest thermal conductivity, the T_h of the platinum electrode can reach 54.5 °C, which is the highest temperature for all the electrodes with different electrode materials. On the other hand, the lower thermal conductivity results in the process of heat transfer from the heating copper wire to the electrode surface to be slow, therefore, the ΔT becomes larger. The ΔT of the platinum electrode can reach 11.9 °C, which is the largest among the different electrode materials. Through the T_h of platinum is the highest, the ΔT is also the largest, leading to a relatively low T_s. Combining the above two factors, the thermal conductivity of gold is moderate, therefore, the T_s is the highest.

Table 1. Fitting equations for different electrode surface temperatures.

T_s (°C)	Fitting Equation	R^2
40	$I = -0.008 + 0.009D_2$	0.9960
60	$I = -0.020 + 0.012D_2$	0.9960
100	$I = -0.028 + 0.0145D_2$	0.9995
120	$I = -0.028 + 0.0154D_2$	0.9999
150	$I = -0.031 + 0.0166D_2$	0.9999

Table 2. Summary of electrode surface temperatures for different electrode materials.

Electrode material	[1]λ ($W \cdot m^{-2} \cdot K^{-1}$)	T_s (°C)	[2]T_h (°C)	[3]ΔT (°C)
Silver	429	44.7	47.6	2.9
Copper	400	44.8	47.9	3.1
Gold	317	45.0	48.7	3.7
Graphite	150	44.5	51.7	7.2
Nickel	90.7	43.5	53.5	10
Platinum	71.6	42.6	54.5	11.9

1. λ represents thermal conductivity of the electrode material. 2. T_h represents the highest temperature inner the electrode. 3. ΔT represents the temperature difference between T_h and T_s.

4. Conclusions

In summary, this report introduces a finite element software (COMSOL) to analyze the factors that influence the surface temperature (T_s). Heat transfer in the inner CHMDEs that work in a three-electrode electrochemical cell is analyzed and modeled. The results are consistent with the measured data for the determination of T_s rise. The simulated results show that the temperature difference between the electrode surface and the bottom of the heated copper wire has a good linear relationship with the square of heating current. Distances between the electrode surface and the bottom of the heated copper wire also exhibited a good linear relationship with T_s. Considering the cost, 25-mm length of the gold wire is enough to obtain a relatively high T_s. In addition, the highest T_s can be obtained when the electrode material is gold and the diameter of the gold disk is 0.2 mm. The relationship of diameters of heated copper wires with currents to obtain different temperatures has also been studied. It is expectable that the simulation results be used to significantly help the design and operation of electrically heated microsensors in practical applications.

Acknowledgements

This work was financially supported by the Key scientific research project of higher education institutions in Henan Province (22A350017).

References

[1] Gründler P, Zerihun T, Möller A, Kirbs A. A simple method for heating micro electrodes *in-situ*[J]. J. Electroanal. Chem., 1993, 360: 309−314.

[2] Grundler P, Zerihun T, Kirbs A, Grabow H. Simultaneous joule heating and potential cycling of cylindrical microelectrodes[J]. Anal. Chim. Acta, 1995, 305(1−3): 232−240.

[3] Zerihun T, Griindler P. Electrically heated cylindrical microelectrodes.The reduction of dissolved oxygen on Pt[J]. J. Electroanal. Chem., 1996, 404: 243−248.
[4] Valdes J L, Miller B. Thermal modulation of rotating disk electrodes: steady-state response[J]. J. Phys. Chem., 1988, 92: 525−532.
[5] Gründler P, Degenring D. The limits of aqueous hot-wire electrochemistry: near-critical and supercritical fluids in electrochemical sensors?[J]. Electroanalysis, 2001, 13: 755−759.
[6] Baranski A S. Hot microelectrodes[J]. Anal. Chem., 2002, 74: 1294−1301.
[7] Wildgoose G G, Giovanelli D, Lawrence N S, Compton R G. High-temperature electrochemistry: a review[J]. Electroanalysis, 2004, 16(6): 421−433.
[8] Gründler P, Flechsig G U. Principles and analytical applications of heated electrodes[J]. Microchim. Acta, 2006, 154(3−4): 175−189.
[9] Grundler P, Kirbs A, Dunsch L. Modern thermoelectrochemistry[J]. Chemphyschem, 2009, 10(11): 1722−1746.
[10] Cutress I J, Marken F, Compton R G. Microwave-assisted electroanalysis: a review[J]. Electroanalysis, 2009, 21(2): 113−123.
[11] Flechsig G U, Walter A. Electrically heated electrodes: practical aspects and new developments[J]. Electroanalysis, 2012, 24(1): 23−31.
[12] Wang J, Grulndler P, Flechsig G U, Jasinski M, Rivas G, Sahlin E, Paz J LL. Stripping analysis of nucleic acids at a heated carbon paste electrode[J]. Anal. Chem., 2000, 72(16): 3752−3756.
[13] Tsai Y C, Coles B A, Compton R G, Marken F. Microwave activation of electrochemical processes: enhanced electrodehalogenation in organic solvent media[J]. J. Am. Chem. Soc., 2002, 124(33): 9784−9788.
[14] Wei H, Sun J J, Guo L, Li X, Chen G N. Highly enhanced electrocatalytic oxidation of glucose and shikimic acid at a disposable electrically heated oxide covered copper electrode [J]. Chem. Commun. 2009;(20): 2842−2844.
[15] Walter A, Surkus A E, Flechsig G U. Hybridization detection of enzyme-labeled DNA at electrically heated electrodes[J]. Anal. Bioanal. Chem., 2013, 405(11): 3907−3911.
[16] Huang Z X, Yang S, Guo J W, Wu S H, Sun J J, Chen G N. Supercooled electrodes[J]. Electrochem. Commun., 2014, 48: 107−110.
[17] Huang Z X, Yang S, Yao F Z, Xu K X, Zhang J F, Wu S H, Sun J J. Alternate hot and cold electrodes[J]. Electrochem. Commun., 2015, 61: 129−133.
[18] Yang S, Huang Z X, Hou X H, Cheng F F, Wu S H, Sun J J. A model for understanding the temperature change of an alternate hot and cold micro-band graphite electrode[J]. Electrochem. Commun., 2016, 68: 71−75.
[19] Yang S, Chen X, Mi Z Z, Chen Z M, Li X D, Sun J J, Wu S H. Temperature-controllable electrodes with a one-parameter calibration[J]. ACS Sens., 2019, 4(6): 1594−1602.
[20] Chen Z M, Wang Y, Du X Y, Sun J J, Yang S. Temperature-alternated electrochemical aptamer-based biosensor for calibration-free and sensitive molecular measurements in an unprocessed actual sample[J]. Anal. Chem., 2021, 93(22): 7843−7850.
[21] Ma B, Wang L, He K, Li D G, Liang X D. A lattice Boltzmann analysis of the electro-thermo convection and heat transfer enhancement in a cold square enclosure with two heated cylindrical electrodes[J]. Int. J. Therm. Sci., 2021, 164: 106885.
[22] Wu S H, Zhu B J, Huang Z X, Sun J J. A heated pencil lead disk electrode with direct current and its preliminary application for highly sensitive detection of luteolin[J]. Electrochem. Commun., 2013, 28: 47−50.
[23] Wu S H, Tang Y, Chen L, Ma X G, Tian S M, Sun J J. Amplified electrochemical hydrogen peroxide reduction based on hemin/g-quadruplex dnazyme as electrocatalyst at gold particles modified heated copper disk electrode[J]. Biosens. Bioelectron., 2015, 73: 41−46.
[24] Wu S H, Zeng Y F, Chen L, Tang Y, Xu Q L, Sun J J. Amplified electrochemical DNA sensor based on hemin/g-quadruplex dnazyme as electrocatalyst at gold particles modified heated gold disk electrode[J]. Sens. Actuator B-Chem., 2016, 225: 228−232.
[25] Wu S H, Zhang B, Wang F F, Mi Z Z, Sun J J. Heating enhanced sensitive and selective electrochemical detection of Hg^{2+} based on T-Hg^{2+}-T structure and exonuclease iii-assisted target recycling amplification strategy at heated gold disk electrode[J]. Biosens. Bioelectron., 2018, 104: 145−151.
[26] Beckmann A, Coles B A, Compton R G, Gründler P, Marken F, Neudeck A. Modeling hot wire electrochemistry. Coupled heat and mass transport at a directly and continuously heated wire[J]. J. Phys. Chem. B, 2000, 104(4): 764−769.
[27] Baranski A S. Hot microelectrodes[J]. Anal. Chem., 2002, 74(6): 1294−1301.
[28] Boika A, Baranski A S. Dielectrophoretic and electrothermal effects at alternating current heated disk microelectrodes[J]. Anal. Chem., 2008, 80: 7392−7400.
[29] Baranski A S, Boika A. Ultrahigh frequency voltammetry: effect of electrode material and frequency of alternating potential modulation on mass transport at hot-disk microelectrodes[J]. Anal. Chem., 2012, 84(3): 1353−1359.
[30] Qiu F, Compton R G, Coles B A, Marken F. Thermal activation of electrochemical processes in a rf-heated channel flow cell: experiment and finite element simulation[J]. J. Electroanal. Chem., 2000, 492(2): 150−155.
[31] Gabrielli C, Keddam M, Lizee J F. Frequency analysis of a temperature perturbation technique in electrochemistry : Part i. Theoretical aspects[J]. J. Electroanal. Chem., 1993, 359(1−2): 1−20.
[32] Gabrielli C. A transfer function approach for a generalized electrochemical impedance spectroscopy[J]. J. Electrochem. Soc., 1994, 141(5): 1147−1157.
[33] Mahnke N, Markovic A, Duwensee H, Wachholz F, Flechsig G U, van Rienen U. Numerically optimized shape of directly heated electrodes for minimal temperature gradients[J]. Sens. Actuator B-Chem., 2009, 137(1): 363−369.
[34] Frischmuth K, Visocky P, Gründler P. On modelling heat transfer in chemical microsensors[J]. Int. J. Eng. Sci., 1996, 34(5): 523−530.
[35] Jenkins D M, Song C, Fares S, Cheng H, Barrettino D. Disposable thermostated electrode system for temperature dependent electrochemical measurements[J]. Sens. Actuator B-Chem., 2009, 137(1): 222−229.

电加热微电极传热模式的结构依赖性研究

李炬 [a,b,*],杨森 [b,c]，孙建军 [c,*]
[a] 河南工贸职业学院，河南 郑州 451191
[b] 郑州大学药学院，河南省肿瘤重大疾病靶向治疗与诊断重点实验室，教育部药物关键制备技术重点实验室，药物安全性评价研究中心，河南 郑州 450001
[c] 福州大学化学学院，教育部食品安全与生物分析科学重点实验室，福建省食品安全分析检测技术重点实验室，福建 福州 350108

摘要

近年来，电加热微电极在电分析化学中得到了广泛的关注。研究表明，在高温下促进质量传输和反应动力学通常会导致电流信号增加。然而，目前还没有关于微电极内部传热的研究，这对于微传感器的设计和操作是必要的。本文利用有限元模拟软件（COMSOL）来分析影响表面温度（T_s）的因素，这对线圈加热的微盘电极的加热能力至关重要。电极表面和加热铜线底部之间的距离也与 T_s（$R^2 = 1$）有良好的线性关系。考虑到成本，25 mm 长的金丝足以获得相对较高的 T_s。此外，当电极材料为金且金盘直径为 0.2 mm 时，可以获得最高的 T_s。本文还研究了不同温度下加热铜线直径与电流的关系。仿真结果有望为电加热微传感器的设计和实际应用提供重要帮助。

关键词：电加热微电极；传热；微盘；线圈加热；模型；COMSOL；温度分布